Proteomic Analysis Indicates that Overexpression and Nuclear Translocation of Lactoylglutathione lyase (GLO1) is Associated with Tumor Progression in Murine Fibrosarcoma

Yufeng Wang

Department of Biochemistry and Functional Proteomics, Yamaguchi University Graduate School of Medicine, Ube, Japan

2014.7

Catalogue

Abstract · · · · · 3

1. INTRODUCTION · · · · · 4

2. MATERIALS AND METHODS · · · · · 6

2 .1 Cell Culture & Sample Preparation · · · · · 6

2.2 2-DE Analysis · · · · · 6

2.3 LC-MS/MS Analysis · · · · · 7

2.4. Western Blotting · · · · · 8

2.5. Immunofluorescence · · · · · 9

2.6. MTS assay · · · · · 10

2.7. Wound healing assay · · · · · 10

2.8. Transient transfection · · · · · 10

3. RESULTS & DISCUSSION · · · · · 12

3.1. Comparative proteomics of QR-32 versus QRsP-11 cells · · · · · 12

3.2. Overexpression of GLO1 is accompanied by HspB1 overexpression · · · · · 13

3.3. Nuclear translocation of GLO1 is related to tumor progression · · · · · 14

3.4. MEK/ERK signaling pathway modulates nuclear translocation of GLO1 · · · · · 15

3.5. U0126 and GLO1 siRNA inhibit cell proliferation and migration in QRsP-11 cells · 16

4. CONCLUSION · · · · · 18

Acknowledgement · · · · · 18

References · · · · · 19

Figure Legends · · · · · 24

Figures · · · · · 27

Abstract

Lactoylglutathione lyase (GLO1), a ubiquitously expressed methylglyoxal (MG) detoxification enzyme, is implicated in the progression of various human malignant diseases. However, the role of GLO1 in the development or progression of murine fibrosarcoma is still unclear. We performed proteomic analysis to identify differences in the intracellular proteins of the regressive tumor cell line QR-32 and the inflammatory cell-promoting progressive tumor cell line QRsP-11 of murine fibrosarcoma by two-dimensional gel electrophoresis combined with mass spectrometry. Seven up-regulated proteins were identified in QRsP-11 compared to QR-32 cells, namely GLO1, annexin A1, adenylate kinase isoenzyme 1, transcription factor BTF3, myosin light polypeptide 6, low molecular weight phosphotyrosine protein phosphatase and nucleoside diphosphate kinase B. Heat shock protein beta-1 (HspB1), a methylglyoxal-adducted protein, is concomitantly over-expressed in QRsP-11 as compared to QR-32 cells. We also found out that GLO1 is translocated into the nucleus to a higher extent in QRsP-11 compared to QR-32 cells, which can be reversed by using a MEK inhibitor (U0126). Moreover, U0126 and GLO1 siRNA can inhibit cell proliferation and migration in QRsP-11 cells. Our data suggests that overexpression and nuclear translocation of GLO1 might be associated with tumor progression in murine fibrosarcoma.

1. INTRODUCTION

Glyoxalase is a ubiquitous enzyme, ubiquitously expressed in all mammalian cells composed of two components called glyoxalase I (GLO1) and glyoxalase II (GLO2), which plays a critical role in the detoxification of methylglyoxal by reducing glutathione and transforming electrophilic reactive α-oxoaldehydes including methylglyoxal into the corresponding non-cytotoxic α-hydroxy acids, as well as tissue maturation and cell death [1]. Implication of GLO1 expression has been revealed in various malignant diseases, including colon, breast, prostate, lung, stomach, ovary, brain, renal and pancreatic cancer [2-6]. Recently, GLO1 has been found to be frequently overexpressed in antitumor agent-resistant human leukemia cells and overexpressed-GLO1 reduced cell apoptosis brought about by the chemotherapeutic drugs etoposide and adriamycin [7]. Moreover, GLO1 has been reported to be up-regulated in human malignant melanoma and to be related to tumor progression [8]. However, the role of GLO1 in development or progression of fibrosarcoma is still unknown.

Two-dimensional gel electrophoresis (2-DE) tandem mass spectrometry (MS) is a powerful tool for identification of biomarkers or therapeutic targets for diseases. We are applying it to validate the candidate tumor markers and also improve the current proteomic method. To investigate whether GLO1 is a potential biomarker for tumor progression of fibrosarcoma, the regressive tumor cell line QR-32 and the inflammatory cell-promoting progressive tumor cell line QRsP-11 of murine fibrosarcoma were performed to be analyzed by two-dimensional gel electrophoresis combined with mass spectrometry.

Regressive and progressive tumor models of murine fibrosarcoma cells have been established in

our previous study [9]. The QR clones have shown weak ability of tumorigenesis and non-metastasis. QR-32 cells regress spontaneously after injection in normal syngeneic mice. The inflammation-associated progressor QRsP clones have the capability of high tumorigenesis and metastasis which were derived from QR-32 cells.

In our preliminary experiments, we reduced the standard difference value (1.5-fold) to 1.2-fold in order to avoid ignoring important minor variations and GLO1 was identified to be upregulated with a factor of 1.27-fold in QRsP-11 compared to QR-32 cells. We also investigated the action of GLO1 in the inflammatory cell-promoting progressive QRsP-11 compared to the regressive QR-32 tumor cell line of murine fibrosarcoma.

2. MATERIALS AND METHODS

2.1. Cell Culture & Sample Preparation

Regressive (QR-32) and progressive (QRsP-11) tumor model of murine fibrosarcoma cells used in this study have been described previously [9]. QR-32 and QRsP-11 were cultured in Eagle's minimum essential medium supplemented with 10% fetal calf serum (inactivated at 56°C for 30 min), sodium pyruvate, non-essential amino acids and L-glutamine, at 37°C, in a humidified 5% carbon dioxide-95% air mixture. Cells were homogenized in lysis buffer (1% NP-40, 1mM sodium vanadate, 1 mM PMSF, 10 mM NaF, 10 mM EDTA, 50 mM Tris, 165 mM NaCl, 10 μg/mL leupeptin, and 10 μg/mL aprotinin) on ice [10]. Suspensions were incubated for 2 h at 4 °C with vigorous shaking, spun down at 15,000 rpm for 30 min, and the supernatants were stored at -80 °C until use. Cells were fractionated by Nuclear and Cytoplasmic Extraction Reagents (78833, PIERCE Biotechnology, Rockford, IL, USA.) The above ways of protein extraction are suitable for running both of 2-DE and Western blot.

2.2. 2-DE Analysis

Isoelectric focusing (IEF) was performed in an IPGphor 3 IEF unit (GE Healthcare, Buckinghamshire, UK) on 7 (or 11) cm, immobilized linear pH gradient, pH 4-7 (or 3-10) linear gradient IPG strips (Bio-Rad, Hercules, CA, USA) at 50 μA/strip. One hundred μg of protein was used for each 2-DE. Protein was dissolved in rehydration buffer [8 M urea, 2% CHAPS, 0.01%

bromophenol blue, 1.2% Destreak reagent (GE Healthcare)] and 0.5% IPG buffer (GE Healthcare) and loaded into the IPGphor strip holder (GE Healthcare). The strips were then focused according to the following program: rehydration for 10 h (no voltage); 0 to 500 V for 4 h; 500 to 1,000 V for 1 h; 1,000 to 8,000 V for 4 h; 8,000 V for 20 min; and the final phase of 500 V from 20,000 to 30,000 Vh. The IPG strips were equilibrated in equilibration buffer 1 (6 M urea, 0.5 M Tris-HCl pH 8.8, 30% glycerol, 2% SDS, 2% 2-ME) and in equilibration buffer 2 (6 M urea, 0.5 M Tris-HCl pH 8.8, 30% glycerol, 2% SDS, 2.5% iodoacetoamide) for 10 min each. The IPG strips were then transferred onto precast polyacrylamide gels with a linear concentration gradient of 4-20% (Bio-Rad) and run at 200 V for 1 h. After running, the gels were fixed in 40% ethanol and 10% acetic acid for more than 2.5 h. The gels were then stained with Flamingo™ Fluorescent Gel Stain (Bio-Rad) overnight for labeling proteins with fluorescence. The stained gels were washed with Milli-Q water 3 times for 5 min and then scanned and analyzed by using the ProXpress 2-D Proteomic Imaging System (PerkinElmer, Waltham, MA, USA) and Progenesis Samespots software (Nonlinear, Newcastle, upon Tyne, UK). The image analysis included steps of spots matching and statistics. The intensity of each spot was normalized by total valid spot volume. Only statistically significant (>1.2 fold; $p<0.05$, ANOVA) spots were determined for further MS analysis. After image analysis, the gels were restained with See Pico™ (Benebiosis, Seoul, Korea) overnight. The selected protein spots that showed differential expression were picked up from the gels and identified by MS analysis. Five gels were repeated for each sample in 2-DE experiment.

2.3. LC-MS/MS Analysis

The gel pieces were destained by rinsing in 60% methanol, 0.05 M ammonium bicarbonate, and 5 mM DTT three times for 15 min. The gel pieces were washed twice in 50% methanol, 0.05 M ammonium bicarbonate, and 5 mM DTT for 10 min. The gel pieces were dehydrated twice in 100% acetonitrile (ACN) for 30 min. Enzyme digestion was performed with an in-gel digestion reagent containing 10 μg/mL sequencing-grade-modified trypsin (Promega, Madison, WI, USA) in 30% ACN, 0.05 M ammonium bicarbonate, and 5 mM DTT at 30 °C for 16 h. Then samples were lyophilized by using Labconco Lyph-lock 1 L Model 77400 (Labconco, Kansas, MO, USA) overnight. Lyophilized samples were dissolved in 15 μL of 0.1% formic acid and analyzed by using the liquid chromatography tandem mass spectrometry (LC-MS/MS) system (Agilent 1100 LC-MSD Trap XCT; Agilent Technologies, Palo Alto, CA, USA). MS data analysis was performed by the Agilent Spectrum Mill MS proteomics workbench against the Swiss-Prot protein database search engine (http://kr.expasy.org/sprot/) and MASCOT MS/MS Ions Search engine (http//www.matrixscience.com/search_form_select.html). The criteria for positive identification of proteins were set as follows: filter by protein score >10.0, and filter peptide by score >8, percentage scored peak intensity (% SPI) > 70.

2.4. Western Blotting

Samples were separated in 10% SDS-PAGE and then transfered onto PVDF membranes at 90 mA for 78 min. The membranes were blocked overnight with TBS containing 5% milk at 4 °C and then incubated with the primary antibody against GLO1 (sc-133144, Santa Cruz Biotechnology), p-ERK (sc-7383, Santa Cruz Biotechnology), lamin A/C (sc-6215, Santa Cruz Biotechnology),

HspB1 (sc-1048, Santa Cruz Biotechnology), α-Tubulin (T5168, Sigma) and actin (sc-1616, Santa Cruz Biotechnology). Membranes were then incubated with the secondary antibody conjugated with horse radish peroxidase (1:10,000) for 1 h at room temperature after three times washing with TBS containing 0.2% Tween-20. The membranes were stained with a chemiluminescent reagent (ImmunoStar Long Detection, Wako, Osaka, Japan) and detected by using the Image Reader LAS-1000 Pro (Fujifilm corporation, Tokyo, Japan).

2.5. Immunofluorescence

For immunocytochemistry, cells were cultured on 15 mm round coverslips in 12 well plates at a density of 10^5 cells per well. Cells on the coverslips were fixed using fresh 3.7% paraformaldehyde in phosphate buffered saline (PBS) for 30 min when they reached 80% confluency. Samples were then washed with PBS, followed by permeabilization with 0.1% Triton X-100 for 15 min. After washing with PBS they were incubated in blocking solution (1% donkey serum in PBS with 0.1% Tween 20) for 1 h at room temperature. Cells were then incubated with a primary antibody against with GLO1 (sc-5970, Santa Cruz Biotechnology) in blocking solution overnight at 4°C. After incubation with primary antibody, cells were rinsed with PBS with 0.1% Tween 20 (PBS-T) and incubated with a secondary antibody for 1 h at room temperature. After washing with PBS-T, their nuclei were counter-stained with 1.43 μM DAPI (4,6'-diamidino-2-phenylindole) for 5 min. Coverslips were washed with PBS-T, then mounted face-down onto microscope slides with Fluoromount (Diagnostic BioSystems, Pleasanton, CA, USA). Confocal images were obtained using Nikon Plan Apo 60X/1.40 objective, BZ-9000 series

(BIOREVO) and BZ-II Viewer software (Keyence, Osaka, Japan) by an operator who was unaware of the experimental condition. All parameters (1360 × 1024 resolution, gain + 12dB, exposure method peak, exposure time) were kept constant within an experiment.

2.6. MTS assay.

The viability of cells was determined by CellTiter 96® AQ_{ueous} One Solution Cell Proliferation Assay (Promega, USA). The cells were seeded on 96-well flat-bottom plates. After 24 hr, the indicated conditions of U0126 or siRNA were treated to the cells. The colorimetric reaction was initiated by adding 3-(4, 5-dimethylthiazol-2-yl)–5-(3-carboxymethoxyphenyl)–2 - (4-sulfophenyl) -2H-tetrazolium, inner salt (MTS) at a concentration of 0.317 mg/mL. The quantity of formazan product as measured by the amount of 490-nm absorbance is directly proportional to the number of living cells in culture. Statistic analysis was using a student's *t*-test.

2.7. Wound healing assay

The cells were seeded on 96-well flat-bottom plates for 24 hr. After indicated treatment, using a sterile 200 μL pipet tip, scratch one wound through the cells. Then take pictures after cells exposure to U0126 or siRNA for a time course. The number of migrated cells was counted by Image J. software. All experiments were repeated for three times.

2.8. Transient transfection

Cells were seeded and incubate at 37° C in a CO_2 incubator until the cells are 60-80% confluent. The cells were transfected with validated human GLO1 siRNA (sc-60704, Santa Cruz Biotechnology) or control siRNA (sc-37007, Santa Cruz Biotechnology) by following a siRNA Transfection Protocol (Santa Cruz Biotechnology).

3. RESULTS & DISCUSSION

3.1. Comparative proteomics of QR-32 versus QRsP-11 cells

In a previous study, progressive QRsP clones were generated from the regressive QR-32 murine fibrosarcoma cells, and they have shown significantly ability of increased tumorigenicity compared to QR-32 cells [11]. Our previous studies have identified several potential biomarkers as shown in Figure 1 (indicated by arrows), which might be related to tumor progression in QRsP-11 [9, 12-14]. However, these biomarkers are not always reliable and proportional to tumor progression. Here, we applied 2-DE gel stain with a fluorescent gel staining, and then differences in the spot intensities between the QR-32 and QRsP-11 cells were analyzed and quantified using Progenesis Samespots software, summarized in Figure 2 A. At least 400 protein spots were matched on each 2-DE gel. Seven up-regulated spots (spots 1-7; n=5) in QRsP-11 as compared to QR-32 cells were displayed on 2-DE gel by >1.2-fold increased intensity (Figure 1). The LC-MS/MS system identified the seven up-regulated protein spots as GLO1 (spot 1), annexin A1 (spot 2), adenylate kinase isoenzyme 1 (spot 3), transcription factor BTF3 (spot 4), myosin light polypeptide 6 (spot 5), low molecular weight phosphotyrosine protein phosphatase (Acp1) (spot 6) and nucleoside diphosphate kinase B (spot 7). Each spot number is the same as those in Figure 1. MS/MS data for these proteins are summarized in Figure 2 B, C and D. Only two of the seven up-regulated proteins (identified as GLO1 and Acp1) were below the 1.5-fold threshold (1.2 to 1.3-fold) (Figure 2 D). GLO1 has been previously shown to be related with tumor progression in human melanoma and gastric cancer [8, 15]. Thus GLO1 might play an important role in tumor

progression in murine fibrosarcoma.

3.2. Overexpression of GLO1 is accompanied by HspB1 overexpression

Heat shock protein 27 (Hsp27) also known as HspB1 in mouse is a chaperone of the small heat shock protein group among α-crystallin, Hsp20 and others [16]. Its functions are involved in thermotolerance [17-19], inhibition of apoptosis [16, 20], regulation of cell development [21], cell differentiation [22] and signal transduction [23]. Methylglyoxal (MG) is one of the side-products in glycolysis and its catabolism is depended on the glyoxalase pathway [1]. Hsp27 is the major MG-modified protein at the C-terminal Arg-188 in cells [24]. Inhibition of MG-modification of Hsp27 causes enhancement of chaperone function and sensitization of the cells to chemotherapeutic drugs-induced apoptosis [24, 25].

We tested if HspB1 expression was upregulated together with the MG detoxification enzyme (GLO1) in QRsP-11 compared to QR-32 cells. Expectedly, Western blot analysis demonstrated that the expression of both HspB1 and GLO1 had significant increases in QRsP-11 compared to QR-32 cells (Figure 3 A and B), indicating that the expression of HspB1 might be responsible for the glycolytic activity and/or GLO1 expression.

TNF-induced phosphorylation of GLO1, a dominant factor for cell death, is depended on protein kinase A and NO-mediated modification of GLO1 [26, 27]. To test those modifications, we compared the isoforms of GLO1 between in QR-32 and QRsP-11 cells by 2-D Western blot. We used the position of the most intense isoform of GLO1 as a reference and have designated this isoform as α, shown in Figure 3 C. A previous study has shown that in TNF-treated cells, isoform

α of GLO1 is phosphorylated and moves toward its nearest acidic isoform [26]. However, no change was observed in the expression profile of the TNF-inducible isoform of GLO1 in either QRsP-11 or QR-32 cells (indicated in Figure 3 C by rectangle). Interestingly, the basic isoform of GLO1 (indicated in Figure 3C by arrow head) was downregulated and the acidic isoforms of GLO1 (indicated in Figure 3 C by asterisk) were upregulated in QRsP-11 compared to QR-32 cells (Figure 3 C). These results suggest that an unknown modification to GLO1, different from the TNF-induced modification [26] occurs during tumor progression in murine fibrosarcoma.

3.3. Nuclear translocation of GLO1 is related to tumor progression

There is evidence showing that metabolic enzymes may perform a second role as transcriptional coregulators, as in the case of glyceraldehyde-3-phosphate dehydrogenase [28], guanosine monophosphate synthase [29] and Inosine monophosphate dehydrogenase [30]. We next tested if nuclear translocation of GLO1 had occurred during tumor progression in murine fibrosarcoma. Western blot demonstrated that GLO1 was upregulated in nuclear extracts of QRsP-11 (not in the cytoplasm) compared to QR-32 cells (Figure 4 A). To confirm this, the nuclear translocation of a small proportion of GLO1 was observed in QRsP-11 compared to QR-32 cells by immunofluorescent microscopy (Figure 4 B). This data indicated that nuclear translocation of GLO1 may play a role in tumor progression of murine fibrosarcoma. We then examined the nuclear isoforms of GLO1 in QRsP-11 cells by 2-D Western blot. This experiment demonstrated that acidic isoforms of GLO1 including isoform α were present in nuclear of QRsp-11, but the basic isoform could not be detected (Figure 4 C). Taken together, these results suggested that the

unknown modification may play a key role in regulating nuclear translocation activity of GLO1. However, this unknown modification could not be identified by immunoprecipitation or 2-DE/LC-MS in this study, with the collection of trace amounts of GLO1 isoform being a major limitation. Recently, GLO1 has been identified to be acetylated at the *N*-terminal in eukaryotes and this N-terminal modification had no impact on enzymatic activity [31, 32]. Protein acetylation is a widespread covalent modification in eukaryotes and involved in both activity and nuclear translocation of transcriptional regulators [33, 34]. Thus, whether the unknown modification is acetylation, whether it has the effect on nuclear translocation of GLO1 and whether GLO1 plays a transcriptional role should be clarified in further studies.

3.4. MEK/ERK signaling pathway modulates nuclear translocation of GLO1

The extracellular signal-regulated kinase (ERK) mitogen-activated protein kinase pathway, also known as the MEK-ERK kinase cascade, has been reported to be activated in various types of cancer and to be strongly associated with cell growth, drug resistance and malignant transformation [35]. Activation of ERK was shown to be increased in QRsP-11 compared to QR-32 cells by Western blot, and it was greatly inhibited in QRsP-11 cells by treatment with the MEK inhibitor U0126 (Figure 5 A). We next checked if the MEK/ERK signaling pathway could be involved in the nuclear translocation of GLO1 in QRsP-11 cells. The expression of GLO1 was significantly downregulated in nuclear extracts of QRsP-11 by treatment with U0126 compared to non-treated cells (Figure 5 B). Immunofluorescent microscopy demonstrated that nuclear translocation of GLO1 in QRsP-11 cells was counteracted by treatment with U0126 (Figure 5 C).

This data indicates that activation of ERK and its effect on nuclear translocation of GLO1 may provide important contributions in the tumor progression of murine fibrosarcoma. Nuclear translocation of GLO1, which has been shown in this study, might be dependent on its modified forms. We next tested if inhibition of ERK activity could have an effect on the modification of GLO1. The 2-D Western blot revealed that U0126 induced upregulation of the basic isoform of GLO1 (indicated in Figure 5 D by arrow head) and reduction of the acidic isoforms (indicated in the same figure by asterisk) in QRsP-11 cells. The TNF-related phosphorylation of GLO1 [26] (indicating in Figure 5 D by rectangle) showed no change after treatment with U0126, suggesting that MEK/ERK regulated the modification and nuclear translocation of GLO1 through a TNF-independent manner.

3.5. U0126 and GLO1 siRNA inhibit cell proliferation and migration in QRsP-11 cells

MTS assay and Wound healing assay were used to analyze cell proliferation and migration after treatment by U0126 and GLO1 siRNA (Figure 6). After exposure to U0126 for 24, 48 and 72 hr, cell survivals were determined. As shown in Figure 6 A, U0126 significantly inhibited cell proliferation compared to the controls. Wound healing assay demonstrated that cell migration was inhibited after exposure to U0126 for a time course (Figure 6 B). Moreover, cell proliferation and migration has also shown to be inhibited by knockdown of GLO1 in QRsP-11 cells (Figure 6 D and 6 E). These data indicated that GLO1 is closely associated with cell proliferation and migration in murine fibrosarcoma.

In summary, our study has clearly shown that GLO1 is overexpressed in the nucleus of QRsP-11 compared to QR-32 cells accompanied by HspB1 expression as seen in the 2-DE, Western blot and immunofluorescent assay and knockdown of GLO1 inhibit cell proliferation and migration in QRsP-11 cells. Thus, GLO1 may play a role in the tumor progression of murine fibrosarcoma. Furthermore, we also showed that the MEK/ERK modulated nuclear translocation of GLO1 may occur through the regulation of a posttranslational modification of GLO1.

4. CONCLUSION

The discovery of therapeutic targets with the ability to inhibit tumor progression would help in the development of new drugs. Currently no reliable therapeutic targets with high sensitivity and specificity for tumor progression of fibrosarcoma are available. In this study, we employed proteomics, immunofluorescent microscopy and GLO1 knockdown assay to show that GLO1 was associated with the tumor progression of murine fibrosarcoma. This is based on our findings that there is a relationship between nuclear translocation of GLO1 and tumor progression. GLO1 expression has been shown to be related to expression of genes involved in metastasis-associated pathways and nuclear translocation of NF-κB and HIF1-α [15]. Thus, the targeting of GLO1 activity to inhibit tumor progression may be useful for development of anti-cancer drugs or therapeutic strategies. Further work will focus on understanting and characterizing the functional potency of GLO1 in gene transcription and tumor progression of murine fibrosarcoma.

Acknowledgement

Thanks to Prof. Kazuyuki Nakamura, Ass. Prof. Yasuhiro Kuramitsu, Dr. Kazuhiro Tokuda, Dr. Futoshi Okada, Dr. Byron Baron; Mrs, Dr. Junko Akada, and Dr. Takao Kitagawa at Department of Biochemistry and Functional Proteomics Yamaguchi University Graduate School of Medicine. Owing to their insightful guidance and comment on my paper as well as patient revising, the completion of this paper is made possible.

References

[1] Thornalley, P. J., The glyoxalase system: new developments towards functional characterization of a metabolic pathway fundamental to biological life. Biochem J. 1990, 269, 1-11.

[2] Ranganathan, S., Walsh, E. S., Godwin, A. K., Tew, K. D., Cloning and characterization of human colon glyoxalase-I. J Biol Chem. 1993, 268, 5661-7.

[3] Rulli, A., Carli, L., Romani, R., Baroni, T. *et al.*, Expression of glyoxalase I and II in normal and breast cancer tissues. Breast Cancer Res Treat. 2001, 66, 67-72.

[4] Davidson, S. D., Cherry, J. P., Choudhury, M. S., Tazaki, H. *et al.*, Glyoxalase I activity in human prostate cancer: a potential marker and importance in chemotherapy. J Urol. 1999, 161, 690-1.

[5] Sakamoto, H., Mashima, T., Sato, S., Hashimoto, Y. *et al.*, Selective activation of apoptosis program by S-p-bromobenzylglutathione cyclopentyl diester in glyoxalase I-overexpressing human lung cancer cells. Clin Cancer Res. 2001, 7, 2513-8.

[6] Wang, Y., Kuramitsu, Y., Ueno, T., Suzuki, N. *et al.*, Glyoxalase I (GLO1) is up-regulated in pancreatic cancerous tissues compared with related non-cancerous. Anticancer Res. 2012, 32, 3219-22.

[7] Sakamoto, H., Mashima, T., Kizaki, A., Dan, S. *et al.*, Glyoxalase I is involved in resistance of human leukemia cells to antitumor agent-induced apoptosis. Blood. 2000, 95, 3214-8.

[8] Bair, W. B. 3rd., Cabello, C. M., Uchida, K., Bause, A. S. *et al.*, GLO1 overexpression in human malignant melanoma. Melanoma Res. 2010, 20, 85-96.

[9] Hayashi, E., Kuramitsu, Y., Okada, F., Fujimoto, M. *et al.*, Proteomic profiling for cancer progression: Differential display analysis for the expression of intracellular proteins between regressive and progressive cancer cell lines. Proteomics. 2005, 5, 1024-32.

[10] Kuramitsu, Y., Harada, T., Takashima, M., Yokoyama, Y. *et al.*, Increased expression and phosphorylation of liver glutamine synthetase in well-differentiated hepatocellular carcinoma tissues from patients infected with hepatitis C virus. Electrophoresis. 2006, 27, 1651-8.

[11] Okada, F., Hosokawa, M., Hamada, J. I., Hasegawa, J. *et al.*, Malignant progression of a mouse fibrosarcoma by host cells reactive to a foreign body (gelatin sponge). Br J Cancer. 1992, 66, 635-9.

[12] Takenawa, T., Kuramitsu, Y., Wang, Y., Okada, F. *et al.*, Proteomic analysis showed down-regulation of nucleophosmin in progressive tumor cells compared to regressive tumor cells. Anticancer Res. 2013, 33, 153-60.

[13] Kuramitsu, Y., Hayashi, E., Okada, F., Zhang, X. *et al.*, Two-dimensional gel electrophoresis using immobilized pH gradient strips and FlamingoTM fluorescent gel stain identified non-nuclear proteins possibly related to malignant tumour progression. Anticancer Res. 2011, 31, 1259-63.

[14] Kuramitsu, Y., Hayashi, E., Okada, F., Tanaka, T. *et al.*, Proteomic analysis for nuclear proteins related to tumour malignant progression: a comparative proteomic study between malignant progressive cells and regressive cells. Anticancer Res. 2010, 30, 2093-9.

[15] Cheng, W. L., Tsai, M. M., Tsai, C. Y., Huang, Y. H. *et al.*, Glyoxalase-I is a novel prognosis factor associated with gastric cancer progression. PLoS One. 2012, 7, e34352.

[16] Acunzo, J., Katsogiannou, M., Rocchi, P., Small heat shock proteins HSP27 (HspB1),

αB-crystallin (HspB5) and HSP22 (HspB8) as regulators of cell death. Int J Biochem Cell Biol. 2012, 44, 1622-31.

[17] Kuramitsu, Y., Wang, Y., Taba, K., Suenaga, S. *et al.*, Heat-shock protein 27 plays the key role in gemcitabine-resistance of pancreatic cancer cells. Anticancer Res. 2012, 32, 2295-9.

[18] Kim, J., Jung, H., Lim, W., Kim, S. *et al.*, Down-regulation of heat-shock protein 27-induced resistance to photodynamic therapy in oral cancer cells. J Oral Pathol Med. 2013, 42, 9-16.

[19] Fuqua, S. A., Oesterreich, S., Hilsenbeck, S. G., Von, Hoff, D. D. *et al.*, Heat shock proteins and drug resistance. Breast Cancer Res Treat. 1994, 32, 67-71.

[20] Concannon, C. G., Gorman, A. M., Samali, A., On the role of Hsp27 in regulating apoptosis. Apoptosis. 2003, 8, 61-70.

[21] Liu, S., Dai, X., Cai, L., Ma, X. *et al.*, Effect of Hsp27 on early embryonic development in the mouse. Reprod Biomed Online. 2013, 26, 491-9.

[22] Mehlen, P., Mehlen, A., Godet, J., Arrigo, A. P., Hsp27 as a switch between differentiation and apoptosis in murine embryonic stem cells. J Biol Chem. 1997, 272, 31657-65.

[23] Ibitayo, A. I., Sladick, J., Tuteja, S., Louis-Jacques, O. *et al.*, HSP27 in signal transduction and association with contractile proteins in smooth muscle cells. Am J Physiol. 1999, 277, G445-54.

[24] Sakamoto, H., Mashima, T., Yamamoto, K., Tsuruo, T., Modulation of heat-shock protein 27 (Hsp27) anti-apoptotic activity by methylglyoxal modification. J Biol Chem. 2002, 277, 45770-5.

[25] Oya-Ito, T., Liu, B. F., Nagaraj, R. H., Effect of methylglyoxal modification and

phosphorylation on the chaperone and anti-apoptotic properties of heat shock protein 27. J Cell Biochem. 2006, 99, 279-91.

[26] Van, Herreweghe, F., Mao, J., Chaplen, F. W., Grooten, J. *et al.*, Tumor necrosis factor-induced modulation of glyoxalase I activities through phosphorylation by PKA results in cell death and is accompanied by the formation of a specific methylglyoxal-derived AGE. Proc Natl Acad Sci U S A. 2002, 99, 949-54.

[27] de, Hemptinne, V., Rondas, D., Vandekerckhove, J., Vancompernolle, K., Tumour necrosis factor induces phosphorylation primarily of the nitric-oxide-responsive form of glyoxalase I. Biochem J. 2007, 407, 121-8.

[28] Zheng, L., Roeder, R. G., Luo, Y., S phase activation of the histone H2B promoter by OCA-S, a coactivator complex that contains GAPDH as a key component. Cell. 2003, 114, 255-66.

[29] van, der, Knaap, J. A., Kozhevnikova, E., Langenberg, K., Moshkin, Y. M. *et al.*, Biosynthetic enzyme GMP synthetase cooperates with ubiquitin-specific protease 7 in transcriptional regulation of ecdysteroid target genes. Mol Cell Biol. 2010, 30, 736-44.

[30] Kozhevnikova, E. N., van, der, Knaap, J. A., Pindyurin, A. V., Ozgur, Z. *et al.*, Metabolic enzyme IMPDH is also a transcription factor regulated by cellular state. Mol Cell. 2012, 47, 133-9.

[31] Ridderström, M., Mannervik, B., Optimized heterologous expression of the human zinc enzyme glyoxalase I. Biochem J. 1996, 314, 463-7.

[32] Birkenmeier, G., Stegemann, C., Hoffmann, R., Günther, R. *et al.*, Posttranslational modification of human glyoxalase 1 indicates redox-dependent regulation. PLoS One. 2010, 5,

e10399.

[33] Ventura, M., Mateo, F., Serratosa, J., Salaet, I. *et al.*, Nuclear translocation of glyceraldehyde-3-phosphate dehydrogenase is regulated by acetylation. Int J Biochem Cell Biol. 2010, 42, 1672-80.

[34] Qiang, L., Banks, A. S., Accili, D., Uncoupling of acetylation from phosphorylation regulates FoxO1 function independent of its subcellular localization. J Biol Chem. 2010, 285, 27396-401.

[35] McCubrey, J. A., Steelman, L. S., Chappell, W. H., Abrams, S. L. *et al.*, Roles of the Raf/MEK/ERK pathway in cell growth, malignant transformation and drug resistance. Biochim Biophys Acta. 2007, 1773, 1263-84.

Figure Legends

Figure 1. Two-dimensional gel electrophoresis images of QR-32 and QRsP-11 stained with Flamingo Gel Staining. Proteins were separated on pH 3-10 linear, immobilized pH gradient strips followed by 5-20% SDS-PAGE. Seven spots as novel candidates showed enhanced intensity on gels of QRsP-11 compared with QR-32. They were numbered spot 1-7. Arrows indicate protein spots which were indentified in previous studies.

Figure 2. Enhanced protein expressions in QRsP-11 compared to QR-32 cells. (A) Different intensity of the spots in QRsP-11 compared to QR-32 cell line was measured by Progenesis Samespots software (n=5). (B) MS and (C) MS/MS spectra of trypsin-digested spot 1. (D) MS data analysis was summarized by the Agilent Spectrum Mill MS proteomics workbench against the Swiss-Prot protein database search engine and MASCOT MS/MS Ions Search engine (n=5). Spot numbers are same as in Fig.1.

Figure 3. Expressions of GLO1 and HspB1 by 1-D and 2-D Western blot. (A) QR-32 and QRsP-11 cells were lysed and resolved by 10% SDS-PAGE and probed with specific antibodies. Actin was used to normalize the loading levels of protein. (B) The expression of HspB1 and GLO1 were tested by western blot and the relative intensity was measured by student-*t* test (n=3). *, p<0.05. Actin was used to normalized loading volume of samples (C) QR-32 and QRsP-11 cells were lysed and resolved on pH 4-7 linear, immobilized pH gradient strips followed by 10% SDS-PAGE and probed with specific antibodies. Arrow indicates the reference isoform α of

GLO1. Rectangle indicates TNF-related phosphorylated isoform of GLO1. Arrowhead indicates the downregulated basic isoform of GLO1 in QRsP-11 compared to QR-32. *, indicates the upregulated acdic isoforms of GLO1 in QRsP-11 compared to QR-32.

Figure 4. Nuclear translocation of GLO1 in tumor progression of murine fibrosarcoma. QR-32 and QRsP-11 cells were fractionated and resolved by SDS-PAGE and probed with specific antibodies. α-Tubulin and Lamin A/C were used as cytoplasmic and nuclear fraction markers, respectively. (B) The indicated cells were stained with specific antibodies against to GLO1 and then detected by confocal microscopy. Red; GLO1, Blue; DAPI. (C) Fractionated-cells were resolved on pH 4-7 linear, immobilized pH gradient strips followed by 10% SDS-PAGE and probed with specific antibodies. Arrow and Arrowhead indicate same as shown in Figure 3 C.

Figure 5. MEK/ERK involved in GLO1 nuclear translocation. (A) The indicated cells were treated with 20 μM of U0126 for 7 hours, and resolved by SDS-PAGE and probed with specific antibodies. Actin was used to normalize the loading levels of protein. (B) QRsP-11 were treated with 20 μM of U0126 for 7 hours and the nuclear fractions were resolved by SDS-PAGE and probed with specific antibodies. Lamin A/C was used as a nuclear fraction marker. (C) The indicated cells were treated with 20 μM of U0126 for 7 hours, stained with specific antibodies against GLO1 and then detected by confocal microscopy. Red; GLO1, Blue; DAPI. (D) U0126-treated or untreated QRsP-11 cells were resolved on pH 4-7 linear, immobilized pH gradient strips followed by 10% SDS-PAGE and probed with specific antibodies. All the symbols indicate the same as shown in Figure 3 C.

Figure 6. GLO1 is associated with proliferation and migration of QRsP-11 cells. Viability of the QRsP-11 cells after exposure to 20 μM of U0126 (A) or transfection with GLO1 siRNA (D) for 0, 24, 48 and 72 hours ($p < 0.05$, n = 3). (C) Knockdown of GLO1 in QRsP-11 cells was confirmed after transfection with GLO1 or control siRNA at 24 hours by Western blot. Scratch wound-healing assay was conducted in 20 μM of U0126-treated cells (B) or GLO1 siRNA-transfected cells (E above). (E below) Migration cells were counted at 48 hours after cells were scratched (($p < 0.01$, n = 3). Values represent mean ± SD.

Figures

Figure 1

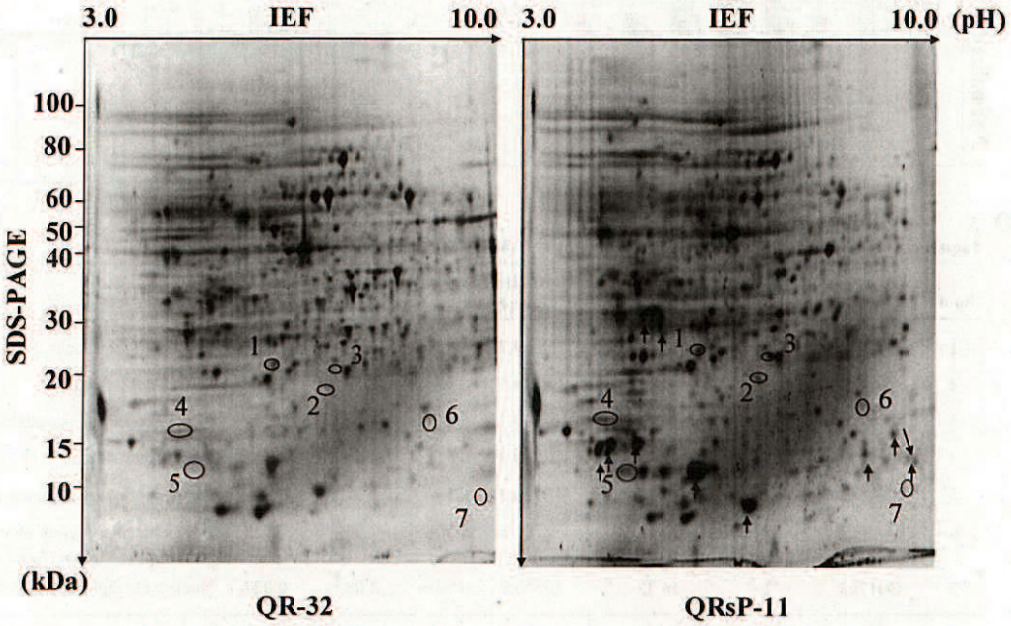

Figure 2

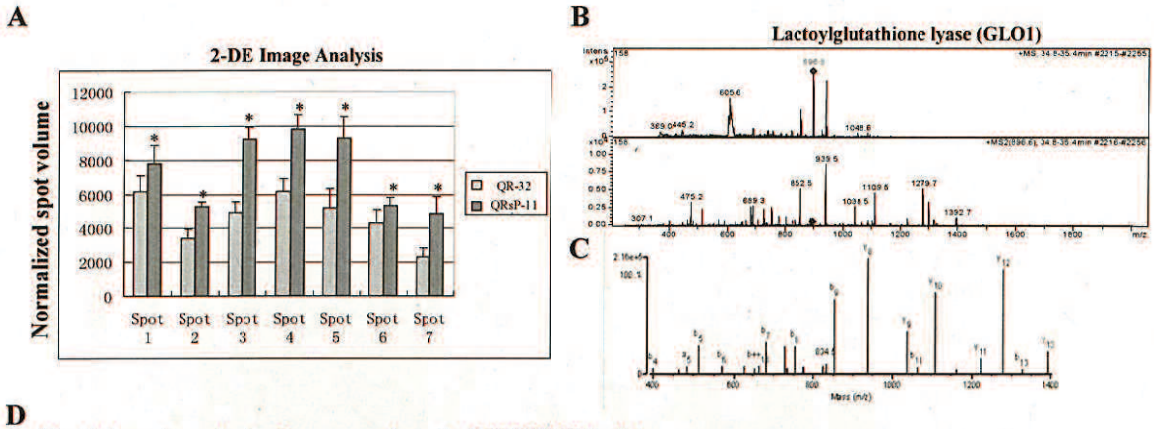

D

Liquid chromatography tandem mass spectrometry (LC-MS/MS) Analysis

Spot	Accession no.	Distinct Peptides	MS/MS Search Score	Molecular Weight (Da)	pI	Ratio of spot intensity	ANOVA *p*-value	Protein
1	Q9CPU0	4	57.42	20809.7	5.24	**1.27** ↑	**0.044**	Lactoylglutathione lyase (**GLO1**)
2	P10107	6	93.41	38734.5	6.97	1.53 ↑	0.049	Annexin A1 (**Anxa1**)
3	Q9R0Y5	5	82.21	21539.7	5.67	1.89 ↑	0.021	Adenylate kinase isoenzyme 1 (**Ak1**)
4	Q64152	3	38.98	22030.9	9.51	1.59 ↑	0.027	Transcription factor BTF3 (**Btf3**)
5	Q60605	2	22.31	16930.2	4.56	1.79 ↑	0.045	Myosin light polypeptide 6 (**Myl6**)
6	Q9D358	2	28.49	18191.8	6.30	1.23 ↑	0.033	Low molecular weight phosphotyrosine protein phosphatase (**Acp1**)
7	Q01768	1	16.33	17363.2	6.97	2.08 ↑	0.027	Nucleoside diphosphate kinase B (**Nme2**)

Figure 3

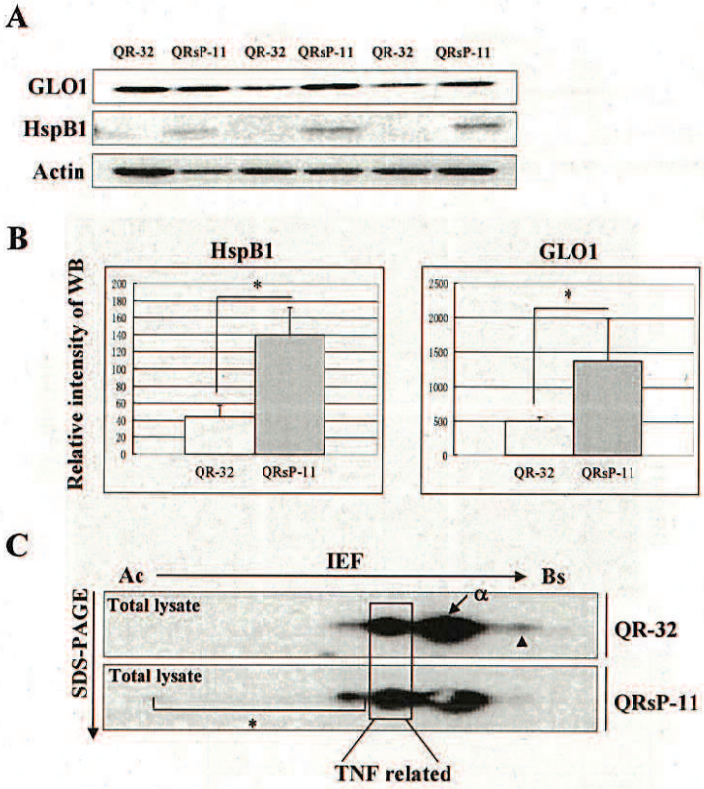
A
QR-32
QRsP-11
QR-32
QRsP-11
QR-32
QRsP-11
GLO1
HspB1
Actin
B
HspB1
GLO1
Relative intensity of WB
QR-32
QRsP-11
QR-32
QRsP-11
C
IEF
Ac
Bs
SDS-PAGE
Total lysate
Total lysate
QR-32
QRsP-11
TNF related

Figure 4

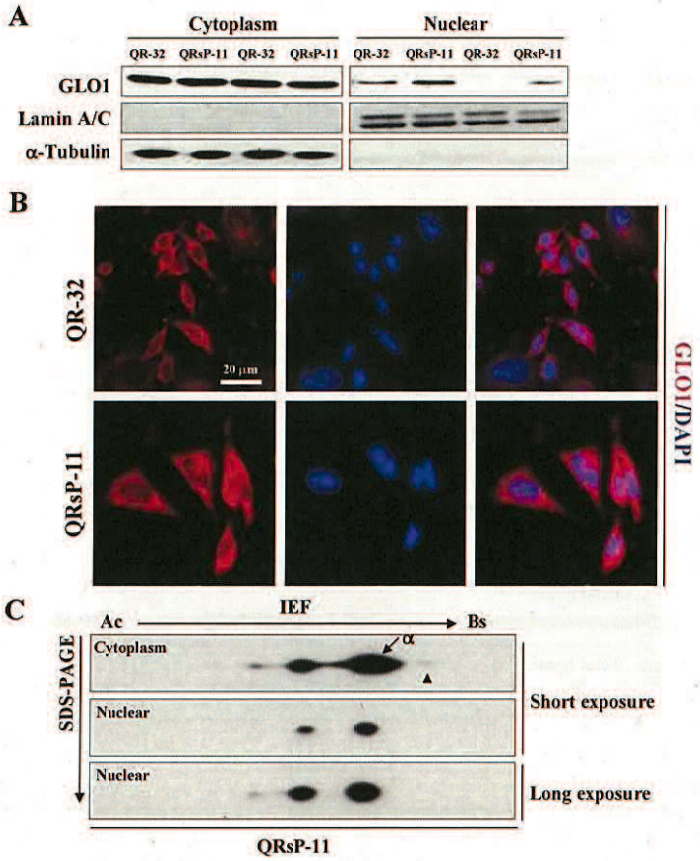
A
Cytoplasm
Nuclear
QR-32 QRsP-11 QR-32 QRsP-11 QR-32 QRsP-11 QR-32 QRsP-11
GLO1
Lamin A/C
α-Tubulin
B
QR-32
QRsP-11
20 μm
GLO1/DAPI
C
IEF
Ac
Bs
SDS-PAGE
Cytoplasm
α
Nuclear
Short exposure
Nuclear
Long exposure
QRsP-11

Figure 5

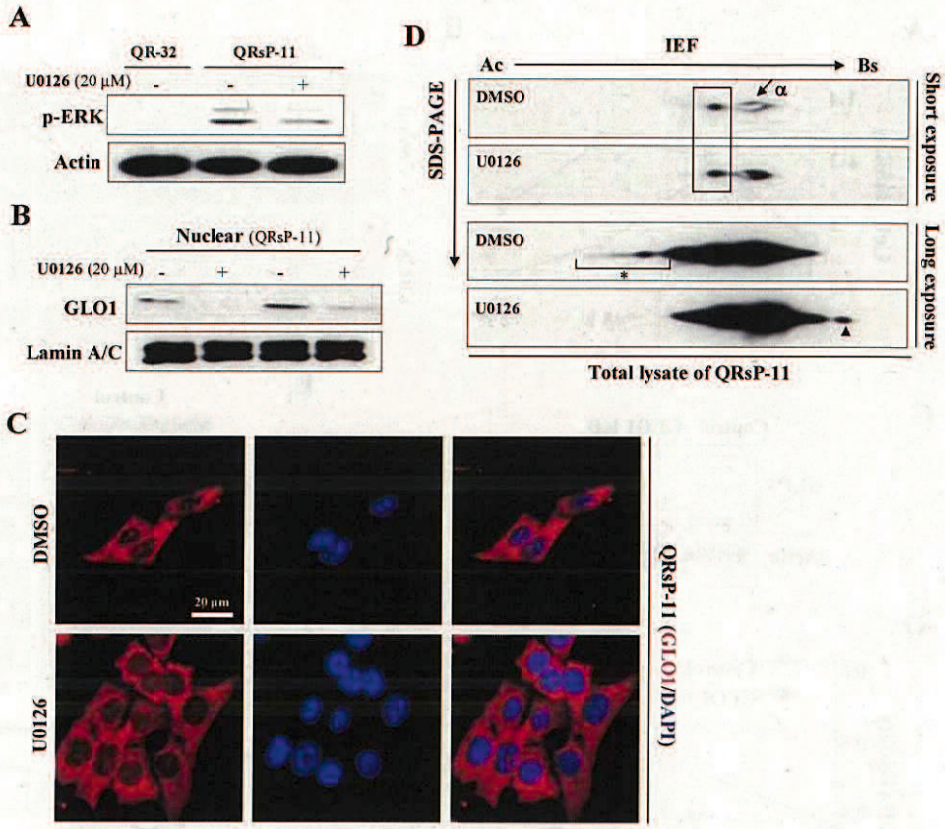
A
QR-32
QRsP-11
U0126 (20 μM) - - +
p-ERK
Actin
B
Nuclear (QRsP-11)
U0126 (20 μM) - + - +
GLO1
Lamin A/C
C
DMSO
U0126
20 μm
QRsP-11 (GLO1/DAPI)
D
IEF
Ac
Bs
SDS-PAGE
DMSO
U0126
α
Short exposure
DMSO
U0126
*
Long exposure
Total lysate of QRsP-11

Figure 6

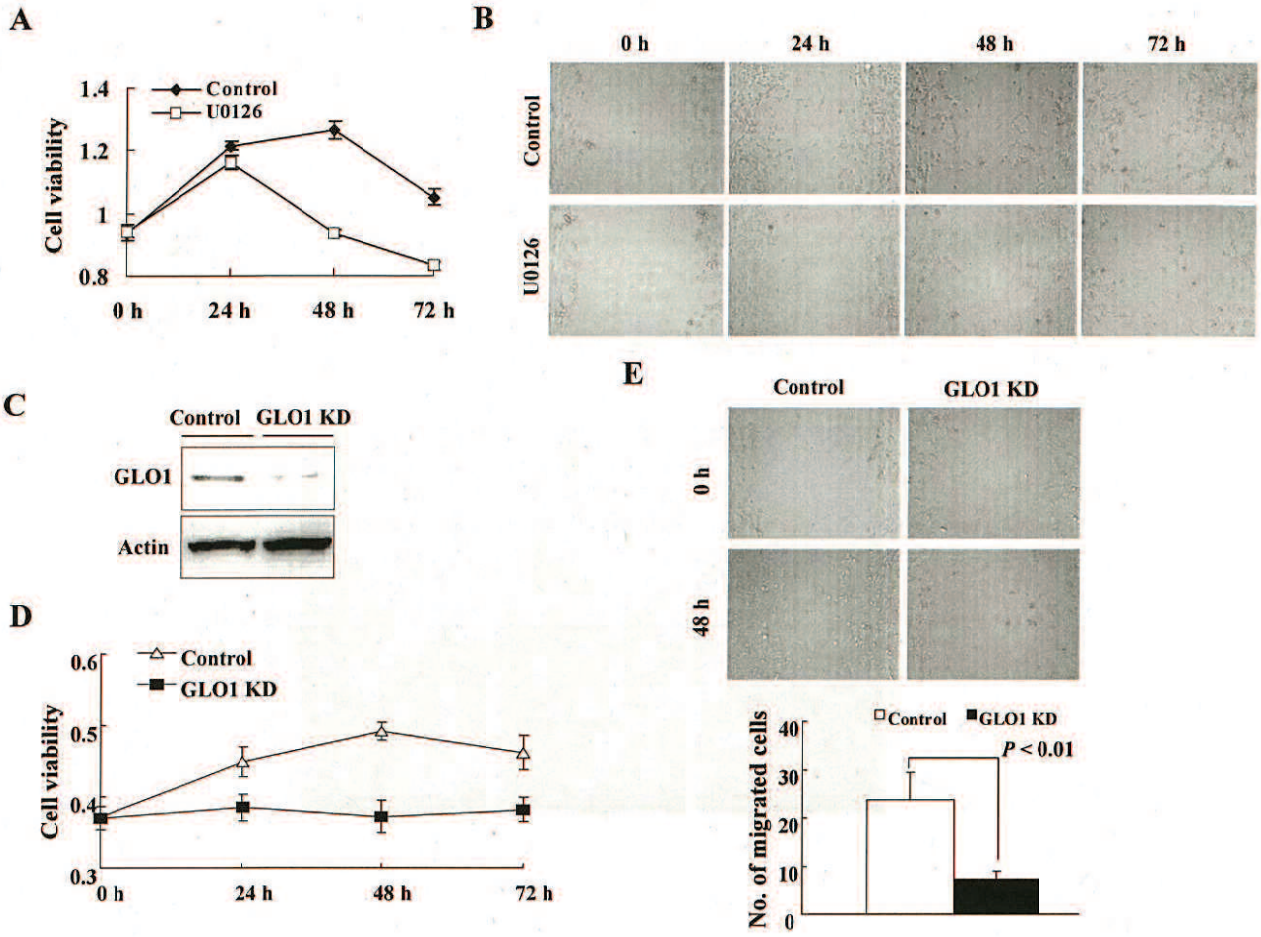
A
Control
U0126
Cell viability
1.4
1.2
1
0.8
0 h
24 h
48 h
72 h
B
0 h
24 h
48 h
72 h
Control
U0126
C
Control
GLO1 KD
GLO1
Actin
D
Control
GLO1 KD
Cell viability
0.6
0.5
0.4
0.3
0 h
24 h
48 h
72 h
E
Control
GLO1 KD
0 h
48 h
Control
GLO1 KD
P < 0.01
No. of migrated cells
40
30
20
10
0